Hindawi Publishing Corporation
Journal of Nanomaterials
Volume 2015, Article ID 874245, 9 pages
http://dx.doi.org/10.1155/2015/874245

Research Article

Cauliflower-Like Co_3O_4/Three-Dimensional Graphene Composite for High Performance Supercapacitor Applications

Huili Liu,[1,2] Xinglong Gou,[2] Yi Wang,[1] Xuan Du,[1] Can Quan,[3] and Tao Qi[1]

[1]*National Engineering Laboratory for Hydrometallurgical Cleaner Production Technology, Institute of Process Engineering, Chinese Academy of Sciences, Beijing 100190, China*
[2]*College of Chemistry and Chemical Engineering, China West Normal University, 1 Shida Road, Nanchong 637000, China*
[3]*Division of Chemistry, National Institute of Metrology, Beijing 100013, China*

Correspondence should be addressed to Yi Wang; wangyi@ipe.ac.cn and Can Quan; superfluidcan@hotmail.com

Received 5 December 2014; Accepted 11 February 2015

Academic Editor: Jiayu Wan

Cauliflower-like Co_3O_4/three-dimensional (3D) graphene nanocomposite material was synthesized by a facile two-step synthesis route (heat reduction of graphite oxide (GO) and hydrothermal synthesis of Co_3O_4). The phase composition, morphology, and structure of the as-obtained products were characterized by scanning electron microscopy (SEM), transmission electron microscope (TEM), and X-ray diffraction (XRD). Electrochemical properties as supercapacitor electrode materials were systematically investigated by cyclic voltammetry (CV) and constant current charge-discharge tests. It was found that the Co_3O_4/3D graphene composite showed a maximum specific capacitance of 863 F g^{-1}, which was obtained by means of CVs at a scan rate of 1 mV s^{-1} in 6 M KOH aqueous solution. Moreover, the composite exhibited improved cycling stability after 1,000 cycles. The good supercapacitor performance is ascribed to the combination of 3D graphene and cauliflower-like Co_3O_4, which leads to a strong synergistic effect to remarkably boost the utilization ratio of Co_3O_4 and graphene for high capacitance.

1. Introduction

With the impending energy crisis, the concerns about the environment are increasing. The research on alternative energy conversion and storage systems which have high efficiency, low cost, and environmental benignity is urgently called for. Supercapacitors, also known as electrochemical capacitors or ultracapacitors, have been intensively investigated in the fields of energy storage and conversion [1, 2]. Compared with the conventional capacitors and secondary batteries, supercapacitors can provide high power density, strong cycle stability, and remarkable pulse charge-discharge properties [1–5]. They are being employed in different applications [1, 6–8], such as mobile electronic devices, back-up power supplies, and hybrid electric vehicles. The charge-storage mechanism in supercapacitor is usually electrical double-layer and Faradic capacitor [7, 9]. The electrical double-layer capacitor (EDLC) roots in charge separation at the electrode/solution interface, whereas the Faradic pseudo-capacitance arises from the reversible redox reactions occurring within the supercapacitor electrode material [10, 11]. As the core component of supercapacitors, electrode material plays an important role in determining the performance of electrochemical capacitors. Recently, tremendous attention has been focused on the development of new materials for supercapacitor electrodes with higher specific capacitance and better cyclic life whilst using environmentally benign materials in easily processable ways.

Among the major materials studied for pseudo-capacitor electrodes, transition metal oxides, such as RuO_2 [12], InO_2 [13], NiO [14], MnO_2 [15], Co_3O_4 [16, 17], and SnO_2 [18], have attracted much attention due to their high theoretical capacities and promising potential. RuO_2 is known as an ideal electrode material for supercapacitors, which shows outstanding electrochemical properties. In some reports, the specific capacitance (SC) of RuO_2, which has a higher

conductivity than carbon materials and remarkable stability, shows as high as 720–768 F g^{-1} [19, 20]. However, the high cost and toxic nature of ruthenium substantially limits its commercial application [21]. Hence, the relatively inexpensive metal oxides have been studied widely. Among them, cobalt oxide is considered as a promising electrode material for supercapacitors due to its relatively low cost, well-defined redox behavior, ultrahigh theoretical SC (~3560 F g^{-1}), and environmental friendliness [22, 23]. For instance, it has been reported that the CoO_x xerogels thermally treated at 150°C showed a good capacitive behavior with a SC value of 291 F g^{-1} [24]. Tummala et al. [7] have synthesized nanostructured Co_3O_4 by plasma spray technique and studied its capacitance properties. The results showed a high SC value of 162 F g^{-1} in 6 M KOH electrolyte.

Graphene, as a new carbon material, has attracted much attention since it was isolated from layer-by-layer graphite in 2004 [25]. It is a promising electrode candidate for EDLCs due to its superb characteristics including the excellent mechanical strength and chemical stability, high electrical and thermal conductivity, and large surface area (a theoretical value of 2630 m^2 g^{-1}) [25]. But the serious agglomeration and restacking between individual graphene sheets result in limited surface utilization percentage and a lower capacitance than the anticipated value [26]. In our recent work [27, 28], three-dimensional (3D) graphene (strictly speaking, it should be reduced graphene oxide (RGO), but it is still called graphene here for convenience) was acquired by heat reduction of graphite oxide in vacuum, which has a higher specific surface area (487 m^2 g^{-1}). Different from Dong's work [29], it has a predominant mesoporosity which centers at 4 nm, and these mesopores can provide a high specific surface area while allowing good mass transport in an electrode process [30].

Recently, many researchers have constructed a graphene-based metal oxide composite structure [17, 31–34]. It was found that these composites showed improved performance with higher electron transport rate, electrolyte contact area, and structural stability. It can be attributed to the special composite structure in which metal oxides are attached on the surface or intercalated into the interlayer of large patches of graphene [31]. Yan et al. [17] reported that graphene nanosheet (GNS)/Co_3O_4 composite has a maximum specific capacitance of 243.2 F g^{-1} at a scan rate of 10 mV s^{-1} in 6 M KOH aqueous solution. However, the composite of 3D graphene which was reported in our previous work [27] and Co_3O_4 has never been investigated so far. Herein, a facile hydrothermal strategy was proposed to deposit cauliflower-like nanostructured Co_3O_4 on 3D graphene nanosheets. Cyclic voltammetry (CV) and galvanostatic charge-discharge measurements were used to assess the electrochemical properties of the Co_3O_4/3D graphene composite in KOH solutions.

2. Experimental

2.1. Materials Preparation. In this study, deionized water was used throughout. Cobalt nitrate hexahydrate ($Co(NO_3)_2{\cdot}6H_2O$), ammonia (37%, $NH_3{\cdot}H_2O$) and potassium hydroxide (KOH) were obtained from Xilong Chemical Engineering Co., Ltd. Hydrochloric acid (37%) and ethanol were supplied by Chemical Plant of Beijing. All the reagents used in this experiment were of analytical grade and without further purification.

Graphene oxide was prepared from nature graphite by a modified Hummers' method. 3D graphene material was obtained by reducing graphite oxide powder in a glass bottle under vacuum followed by heating to 250°C from room temperature [27].

Co_3O_4/3D graphene composite was synthesized as follows. First, 15 mg of 3D graphene was dispersed in 15 mL ethanol with the assistance of ultrasonication for 60 min. Then, 0.5 mmol $Co(NO_3)_2{\cdot}6H_2O$ and 34 μL of 37% ammonia were added to the 3D graphene suspension simultaneously. The as-obtained mixture was magnetically stirred for 20 min. After that, the above suspension was loaded into a 25 mL of Teflon-lined stainless steel autoclave and heated at 170°C for 5 h. The obtained black products were washed by centrifugation for several times using ethanol and deionized water to remove excess ions and then dried in a vacuum oven at 60°C. Afterwards, the material was calcined at 350°C for 3 h in air and then cooled to room temperature. For comparison, Co_3O_4 was also prepared by the same steps without the addition of 3D graphene.

2.2. Characterization Methods. The crystallographic structures of the samples were determined by X-ray diffraction system (XRD, X' Pert-PRO MPD) equipped with Cu K_α (λ = 1.5406 Å) radiation. The morphological analysis was conducted using scanning electron microscope (SEM, JEOL JSM-6700F) and transmission electron microscope (TEM, JEOL JEM-2011, 200 kV). The specific surface area and pore volume of the samples were determined by analyzing the standard nitrogen adsorption isotherm measured at 77 K. An electrochemical workstation system (CHI760D, Chenhua, Shanghai) was employed to study the electrochemical properties. The electrodes were fabricated by mixing 80 wt% active materials, 15 wt% acetylene black, and 5 wt% polyvinylidene fluoride (PVDF) as binder. The mixtures were well blended using alcohol, coated the paste onto nickel foam current collectors (1 cm × 1 cm), were dried at 100°C for 10 h, and were pressed under 20 MPa for 3–5 min. Each electrode contains 2-3 mg active materials. A conventional three-electrode system was employed to investigate the capacitive behaviors. Platinum foil and Hg/HgO (1 M KOH aqueous solution) electrodes were used as the counter and reference electrodes, respectively.

3. Results and Discussion

3.1. Structure and Morphology of the Samples. The XRD patterns of 3D graphene, Co_3O_4, and the as-prepared composite before and after calcination were shown in Figure 1. For 3D graphene, a broad peak was observed at 25.6°, which is attributed to the C (002) plane [31, 35]. The main peaks in the XRD pattern of pure Co_3O_4 (JCPDS, number 42-1467) are located at 19.0, 31.3, 36.8, 44.8, 59.4, and 65.3°, which are

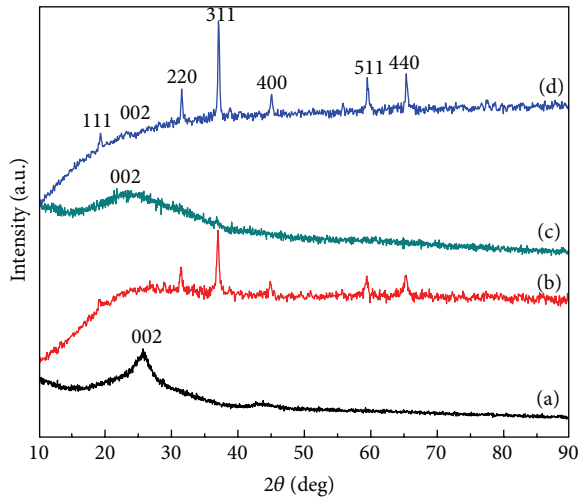

FIGURE 1: XRD patterns of (a) 3D graphene, (b) Co_3O_4, (c) the composite without calcination treatment, and (d) the composite after calcination treatment.

assigned to the crystal planes of (111), (220), (311), (400), (511), and (440) [36]. From Figure 1(c), it can be found that the XRD pattern of the as-prepared composite before calcination does not show any other peak except a broad hump at 2θ of about 25.6° which is attributed to the diffraction peak of C (002) in 3D graphene [35]. However, several peaks appear at 2θ of around 19°, 31°, 37°, 45°, 59°, and 65° obviously in the XRD pattern after calcination. These diffraction peaks are assigned to the crystal planes of (111), (220), (311), (400), (511), and (440), which agree with the typical spinel Co_3O_4 [36]. Thus, the chemical reactions in the synthetic process are supposed as follows:

$$Co(NO_3)_2 + 2NH_3 \cdot H_2O \longrightarrow Co(OH)_2 + 2NH_4^+ + 2NO_3^- \quad (1)$$

$$6Co(OH)_2 + O_2 \longrightarrow 2Co_3O_4 + 6H_2O \quad (2)$$

The absence of diffraction peaks of $Co(OH)_2$ in Figure 1(c) may result from the amorphous state of $Co(OH)_2$. It is inferred that the composite before calcination consists of $Co(OH)_2$ and graphene.

Additionally, from the XRD pattern of the composite after calcination, the characteristic peak of 3D graphene for C (002) is also found. Based on these results, the as-obtained calcinate material can be undoubtedly identified as Co_3O_4/3D graphene composite. Moreover, it is notable that the C (002) peaks in Figures 1(c) and 1(d) shift toward left as compared to that in Figure 1(a), which indicates that $Co(OH)_2$ and Co_3O_4 may lead to the increase of the unit cell volume of graphene because the shift of entire diffraction peaks toward lower 2θ usually suggests the increase of unit cell volume.

The morphology of the as-prepared materials was investigated by SEM, as shown in Figure 2. The graphene material has a 3D structure composed of homogeneous micrometer-sized flakes (Figure 2(a)). Moreover, according to our previous work [27], the 3D graphene material has mesoporosity centered at 4 nm, demonstrating that it belongs to mesoporous materials. Figure 2(b) shows the SEM image of the composite before calcination (i.e., the precursor of Co_3O_4/3D graphene composite). It can be seen that the graphene skeleton maintains structural integrity except that the Co_3O_4 particles are distributed over the graphene surface. After the calcination treatment, it seems that the morphology and structure are similar to those of the precursor of the composite (Figure 2(c)). The high-magnification SEM image in Figure 2(d) reveals that many small Co_3O_4 granules agglomerated together to form some big circular particles with nonuniform diameters from 50 to 250 nm. However, from Figures 2(e) and 2(f), it is clearly seen that, without the addition of 3D graphene, Co_3O_4 and its precursor display cubic morphology, and these particles have a size about 50–100 nm and were stacked irregularly. It indicates that the morphology of Co_3O_4 in the composite material is different from that of pure Co_3O_4. This may be because of the effects of the electrostatic adsorption and other chemical bonds between the oxygen-containing functional groups on the surface of 3D graphene and the precursor of Co_3O_4.

TEM images of Co_3O_4 and Co_3O_4/3D graphene composite are shown in Figure 3. Figures 3(a) and 3(b) display the TEM images of pure Co_3O_4 with different magnification. It can be found that the pure Co_3O_4 sample is composed of a great deal of irregular cubic particles. However, Figure 3(c) reveals that, in the Co_3O_4/3D graphene composite, many nearly spherical Co_3O_4 particles are attached onto 3D graphene nanosheets, which is similar to the results of SEM. Furthermore, it can be seen that the Co_3O_4 cubic particles with a size about 50–100 nanometers are complete and solid from the inset of Figure 3(a). However, from the high magnification TEM image of Co_3O_4/3D graphene composite shown in Figure 3(d), it can be found that the big spherical Co_3O_4 particles in the composite are composed of numerous assembled nanoparticles with a size of 10–25 nanometers, and these small nanoparticles assemble together to display cauliflower-like morphology. This can lead to abundant pore structures, which is beneficial to the electrochemical utilization of metal oxides and the passing of the ions in the electrolyte. Additionally, the HRTEM image of the composite is presented in the inset of Figure 3(d). The Co_3O_4 exhibits high crystallinity and the lattice spacing of 0.26 nm is corresponding to the interspacing of the (311) planes [35].

Nitrogen isotherms of Co_3O_4 and Co_3O_4/3D graphene composite are presented in Figure 4. It is interesting to see that the composite adsorbs much more N_2 than pure Co_3O_4. It suggests that the structural characteristics change greatly after the addition of 3D graphene. The BET surface area increases from 0.111 to 69.7 $m^2\,g^{-1}$ while the pore volume increases from 0.0016 to 0.17 $cc\,g^{-1}$. This is the normal sequence since 3D graphene possesses a large specific surface area and pore volume, and the cauliflower-like morphology of Co_3O_4 in the composite further contributes to the surface area and pore volume.

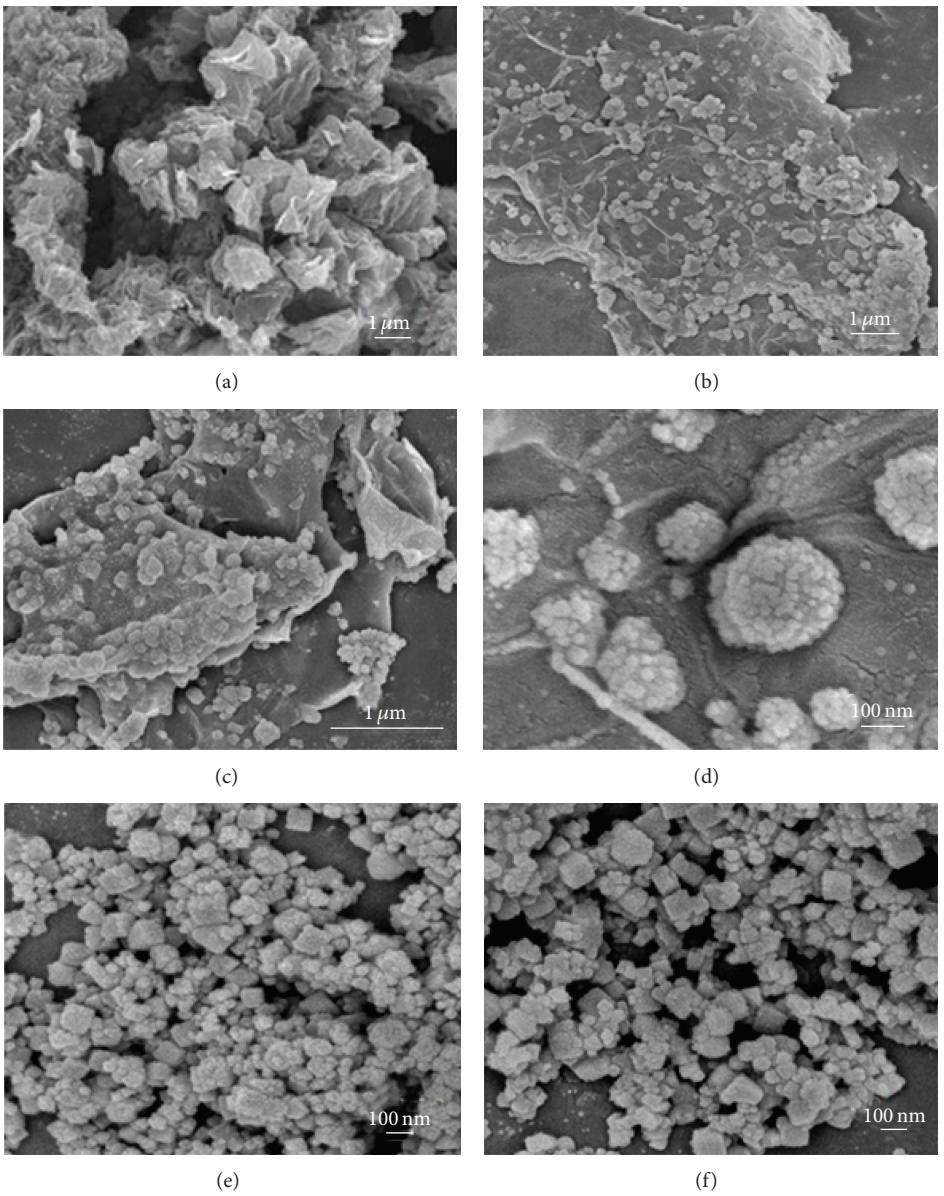

Figure 2: SEM images of (a) 3D graphene, (b) the precursor of Co_3O_4/3D graphene composite, Co_3O_4/3D graphene composite with (c) low and (d) high magnification, and (e) the precursor of Co_3O_4 and (f) Co_3O_4.

3.2. Electrochemical Properties. For potential supercapacitor applications, the capacitor behaviors of the electrodes were examined.

3.2.1. Cyclic Voltammetry (CV). Figure 5(a) displays the CV curves of Co_3O_4/3D graphene composite, Co_3O_4, and 3D graphene at a scan rate of 10 mV s^{-1} in 1 M KOH electrolyte within the potential window of −0.2–0.5 V. Evidently, the area surrounded by the CV curve is dramatically enhanced by the introduction of Co_3O_4 nanoparticles onto 3D graphene sheets as shown in Figure 5(a). This result indicates a large specific capacitance associated with the composite electrode. The CV curves are different from the ideal rectangular shape of the typical electric double-layer capacitance. Unlike 3D graphene, two pairs of redox reaction peaks are visible in the CV curve of the composite, which can be ascribed to the redox process of Co_3O_4, suggesting that the capacitance mainly results from the pseudocapacitance of Co_3O_4. The mechanism of electrochemical reactions of Co_3O_4 in alkaline electrolyte can be expressed as the following equations [36]:

$$Co_3O_4 + OH^- + H_2O \Longleftrightarrow 3CoOOH + e^- \quad (3)$$

$$CoOOH + OH^- \Longleftrightarrow CoO_2 + H_2O + e^- \quad (4)$$

The SC of the electrode, based on CV curves, can be calculated as

$$C = \frac{\left(\int IdV\right)}{\nu m V}, \quad (5)$$

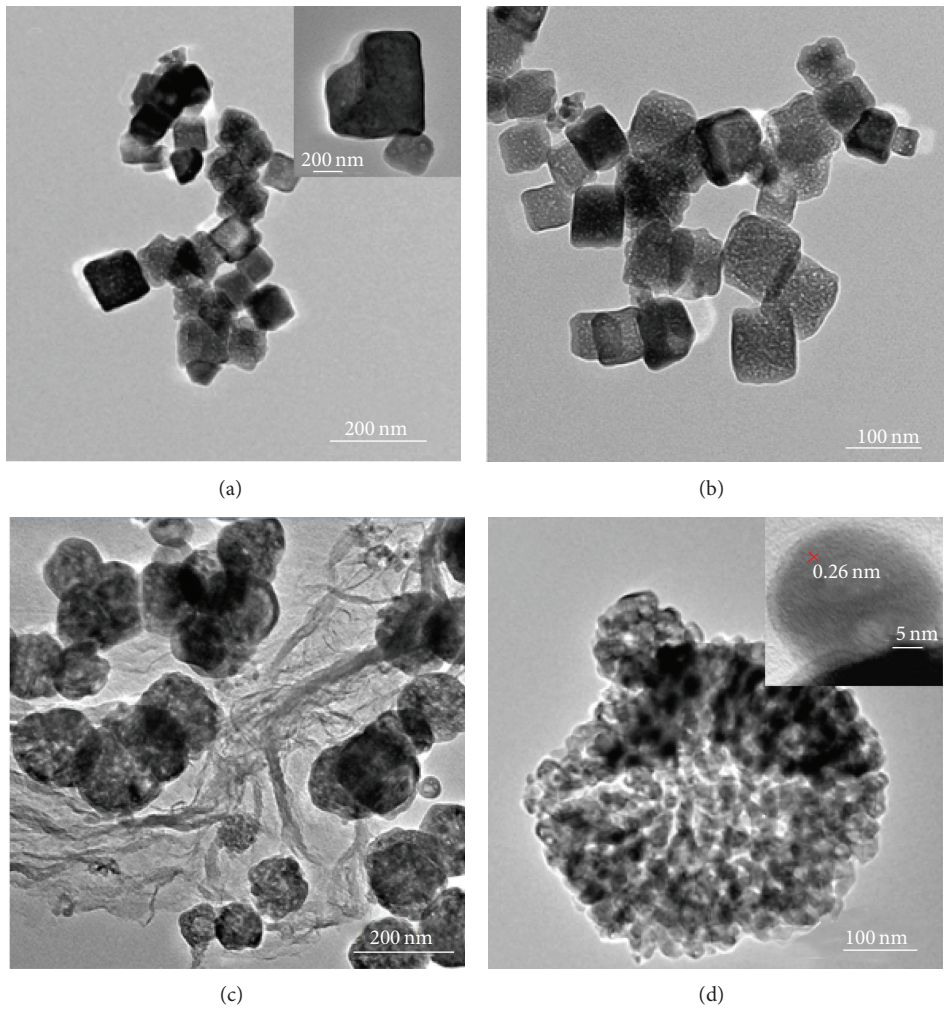

FIGURE 3: TEM images of Co_3O_4 with (a) low and (b) high magnification and Co_3O_4/3D graphene composite with (c) low and (d) high magnification. Inset: high resolution TEM (HRTEM) images.

where C is the SC of electroactive materials ($F\,g^{-1}$), I is the response current (A), V is the potential (V), ν is the potential scan rate ($V\,s^{-1}$), and m is the mass of the electrode materials (g). According to (5), the SCs of the Co_3O_4/3D graphene composite, Co_3O_4, and 3D graphene electrodes are calculated to be about 457, 134, and 97 F/g at a scan rate of 10 $mV\,s^{-1}$, respectively. If the SCs are represented by volumetric capacitance, these values are 965, 335, and 103 F/cm^3, respectively. Clearly, the SC of the composite is not simple sum of Co_3O_4 and 3D graphene but significantly larger than expected. Moreover, the SC value is much higher than that of a Co_3O_4/reduced graphene oxide scrolled structure (163.8 F/g) reported recently [31]. The desirable performance could be attributed to the synergistic effect between graphene sheets and Co_3O_4 nanoparticles in the nanocomposite [37]. This effect may be associated with the fact that conductive graphene is hydrophobic, while Co_3O_4 is hydrophilic but has poor conductivity. It is very likely that Co_3O_4 increases the graphene hydrophilicity for significantly increased utilization of the porous electrode and the conductive graphene enhances the charge transfer rate of Co_3O_4 for higher pseudocapacitance. Furthermore, the large specific surface area and pore volume resulting from the cauliflower-like morphology of Co_3O_4 in the composite may also increase the utilization of Co_3O_4 and thus further enhance the pseudocapacitance. These factors result in a much larger SC value of the composite than the sum of that of 3D graphene and Co_3O_4. Additionally, as compared to two-dimensional (2D) graphene which has been reported [38], 3D graphene has a much higher specific surface area ($487\,m^2\,g^{-1}$) and larger pore volume ($1.04\,cc\,g^{-1}$) [27]. The 3D graphene has predominant mesoporosity which centers at 4 nm, which is in favor of improving the electrochemical accessibility of electrolyte ions and providing preferable EDLCs [30]. Both the pseudocapacitance derived from the cauliflower-like Co_3O_4 and the superior surface and pore properties of 3D graphene contribute to the high capacitance.

Figure 5(b) shows the variation of the calculated SC values of Co_3O_4/3D graphene composite as a function of scan rates in different concentration KOH electrolytes. Obviously,

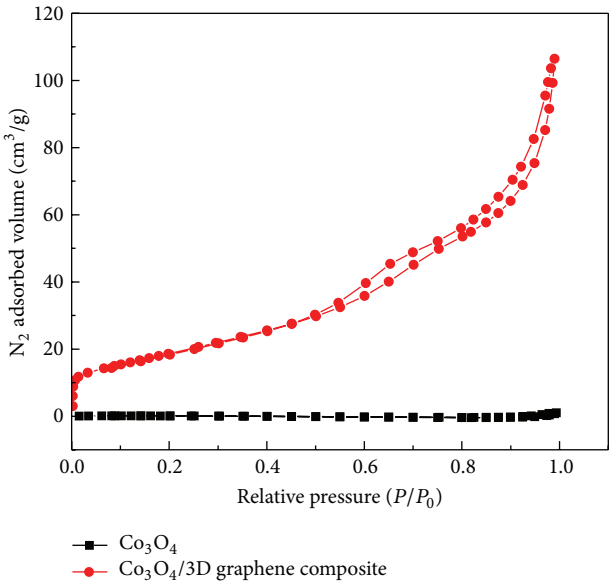

FIGURE 4: N_2 adsorption-desorption isotherms of Co_3O_4 and Co_3O_4/3D graphene composite.

the SC values of the composite decrease gradually with the increase of scan rate. This may be because, at high scan rates, diffusion limits the movement of electrolyte ions due to the time constraint, and only the outer active surface is utilized for charge storage. At lower scan rates, however, all the active surface area can be utilized for charge storage and the electrochemical utilization of Co_3O_4 [39]. As shown in Figure 5(b), 6 M electrolyte provided the largest SC values. The maximum SC value is 863 F g^{-1} in 6 M KOH electrolyte at a scan rate of 1 mV s^{-1}. According to the equations of the electrochemical reactions of Co_3O_4 in alkaline electrolyte, there is OH^- in the reactions. Thus, a high concentration of hydroxyl ions is in favor of increasing the reaction rate. This results in the largest SC value in 6 M KOH solution.

3.2.2. Galvanostatic Charge-Discharge Measurement. Furthermore, galvanostatic charge-discharge measurement was utilized to study the capacitor performance of the as-prepared samples.

Figure 6 depicts the charge-discharge behaviors of Co_3O_4, 3D graphene, and the Co_3O_4/3D graphene composite electrodes between 0 and 0.5 V at a constant current density of 5 A g^{-1} in 1 M KOH aqueous solution. From the charge-discharge curves of 3D graphene, it is evidently seen that the voltage decreases linearly along the discharge time, which shows an ideal double-layer capacitive behavior. However, the discharge curve of Co_3O_4/3D graphene composite consists of a slow potential drop from 0.5 to 0.2 V and a sudden potential decay from 0.2 to 0 V. The latter indicates short charge/discharge duration, which is a pure double-layer capacitance behavior from the charge separation at the electrode/electrolyte interface. However, the former is a typical pseudocapacitance behavior, caused by electrochemical adsorption/desorption or a redox reaction at the electrode/electrolyte interface [40]. Usually, Faradaic redox reaction is accompanied by the double-layer charge-discharge process, and thus the combination of electric double-layer capacitance and Faradaic pseudocapacitance is responsible for the longer charge/discharge duration [17].

From the discharge curves, SC could also be calculated using the following equation:

$$C = \frac{(I\Delta t)}{(m\Delta V)}, \tag{6}$$

where C is the SC of the active materials (F g^{-1}), I, Δt, ΔV, and m are constant discharge current (A), discharge time (s), the voltage change after a full discharge (V), and the mass of the active material (g), respectively [41]. The SC values calculated from the galvanostatic charge and discharge curves are 40, 46, and 337 F g^{-1} for 3D graphene, Co_3O_4, and the composite, respectively, which are similar to the trend of those calculated from CVs. A larger specific capacitance value of 402 F g^{-1} for the composite is obtained at 0.5 A g^{-1}. The much larger SC value of the composite than the sum of that of graphene and pure Co_3O_4 further proves that the combination of 3D graphene and cauliflower-like Co_3O_4 is very beneficial to improving the supercapacitor performance.

Subsequently, the galvanostatic charge-discharge properties of the composite are investigated with different current density in different concentration of KOH electrolytes. The SC values are calculated in accordance with (6) and listed in Table 1. It is found that the SC of the electrode based on the as-prepared composite reached a maximum value of 522 F g^{-1} in 6 M KOH electrolyte at the current density of 0.5 A g^{-1}. The results are similar to the results obtained from the CVs, further indicating that a high concentration of hydroxyl ions is in favor of increasing the reaction rate.

To investigate the cycling performance of the Co_3O_4/3D graphene composite, the charge-discharge tests were performed at 2 A g^{-1} for 1,000 cycles. Figure 7 shows the results of cycling stability measurement. After 1,000 cycles, the specific capacitance of the Co_3O_4/3D graphene composite decreased apparently. An initial total capacitance of 75% was retained after the 1000th discharge cycle. The decay of capacitance can be ascribed to the increased impedance with increasing number of cycles, and it is inferred that the increased impedance could be due to fatigue of the active material during cycling [7]. As compared to some nanostructured Co_3O_4 electrodes reported recently [7], the retention rate of capacitance of the Co_3O_4/3D graphene composite was improved a little, which may be attributed to the special structure of 3D graphene and cauliflower-like Co_3O_4. During cycling, the three-dimensional nanoporous structure of 3D graphene, as well as the cauliflower-like morphology of Co_3O_4, can inhibit the volume change and detachment of Co_3O_4 particles more effectively and thus result in a better cyclic life.

4. Conclusions

In this work, a Co_3O_4/3D graphene composite was synthesized via a facile two-step synthesis route (heat reduction

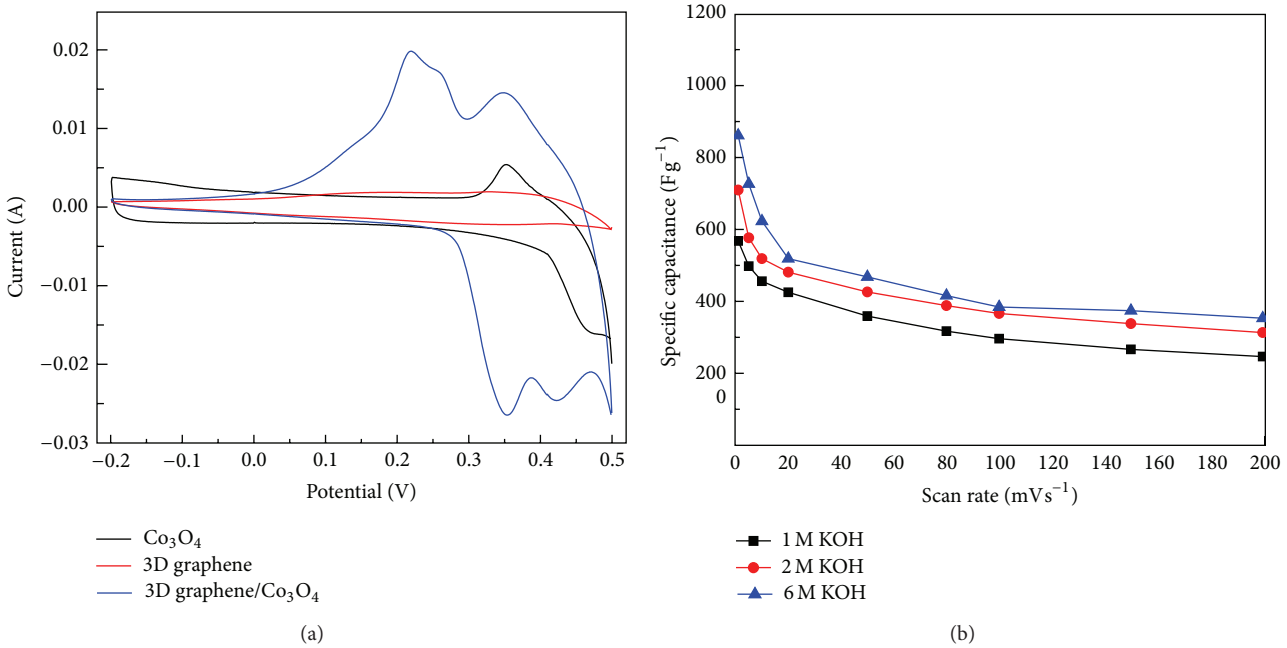

FIGURE 5: (a) CV curves of 3D graphene, Co_3O_4, and Co_3O_4/3D graphene composite at a scan rate of 10 mV s^{-1}, (b) the SC of Co_3O_4/3D graphene composite at various scan rates of 1, 5, 10, 20, 50, 80, 100, and 200 mV s^{-1} within the potential window of −0.2–0.5 V.

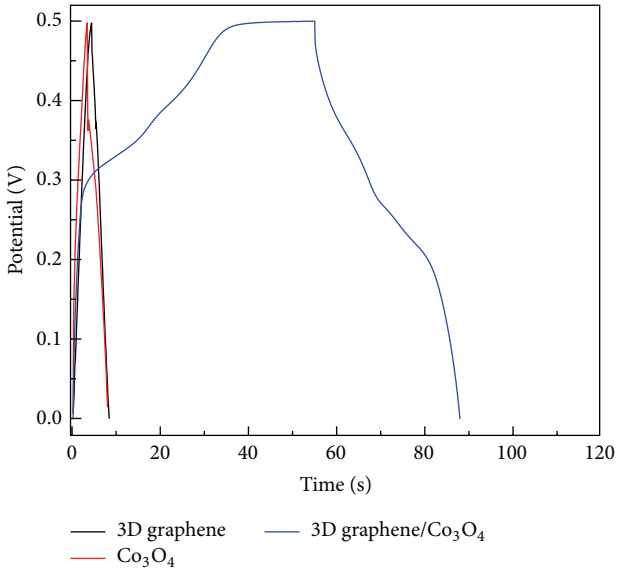

FIGURE 6: Galvanostatic charge/discharge curves of 3D graphene, Co_3O_4, and Co_3O_4/3D graphene composite at a current density of 5 A g^{-1}.

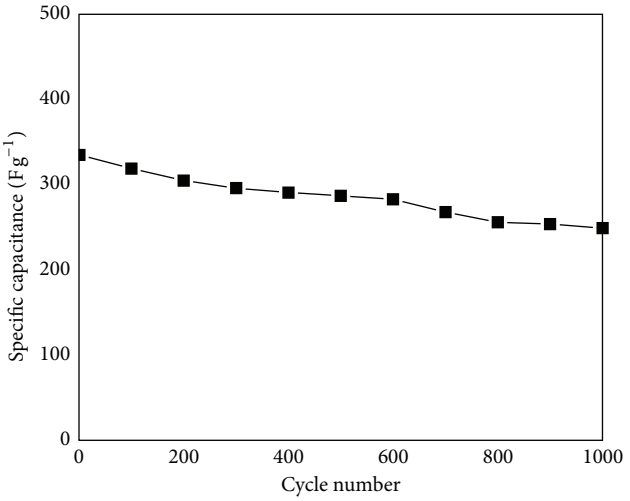

FIGURE 7: Cycling stability measurement result of Co_3O_4/3D graphene composite within the potential window of 0–0.50 V (versus Hg/HgO) at a current density of 2 A g^{-1}.

of GO and hydrothermal synthesis of Co_3O_4). SEM and TEM images showed that, in the composite, many small nanoparticles with a size of 10–25 nm assemble together to display cauliflower-like morphology. The supercapacitor performance of the composite, 3D graphene, and Co_3O_4 was investigated and compared by CV and constant current charge-discharge tests. It was found that the composite showed much larger specific capacitance than the sum of that of 3D graphene and Co_3O_4. Moreover, the composite exhibited better cycling stability. The good supercapacitor performance is ascribed to the combination of 3D graphene and cauliflower-like Co_3O_4, which leads to a strong synergistic effect to remarkably boost the utilization ratio of Co_3O_4 and graphene. The cauliflower-like Co_3O_4/3D graphene composite is believed to be a promising electrode material for supercapacitors.

Table 1: SC values ($F\,g^{-1}$) of Co_3O_4/3D graphene composite at different current density in different concentration electrolytes within the potential window of 0–0.5 V.

	1 M KOH	2 M KOH	6 M KOH
$0.5\,A\,g^{-1}$	402	458	522
$1\,A\,g^{-1}$	380	431	478
$5\,A\,g^{-1}$	337	367	396
$10\,A\,g^{-1}$	296	338	363

Conflict of Interests

The authors declare that there is no conflict of interests regarding the publication of this paper.

Acknowledgments

The authors are grateful for the financial support by One Hundred Talent Program of Chinese Academy of Sciences as well as by the NSFC (51302264) of China.

References

[1] P. Simon and Y. Gogotsi, "Materials for electrochemical capacitors," *Nature Materials*, vol. 7, no. 11, pp. 845–854, 2008.

[2] J. Yan, Z. Fan, W. Sun et al., "Advanced asymmetric supercapacitors based on $Ni(OH)_2$/graphene and porous graphene electrodes with high energy density," *Advanced Functional Materials*, vol. 22, no. 12, pp. 2632–2641, 2012.

[3] L. H. Bao, J. F. Zang, and X. D. Li, "Flexible Zn_2SnO_4/MnO_2 core/shell nanocable-carbon microfiber hybrid composites for high-performance supercapacitor electrodes," *Nano Letters*, vol. 11, no. 3, pp. 1215–1220, 2011.

[4] L. T. Lam and R. Louey, "Development of ultra-battery for hybrid-electric vehicle applications," *Journal of Power Sources*, vol. 158, no. 2, pp. 1140–1148, 2006.

[5] M. Winter and R. J. Brodd, "What are batteries, fuel cells, and supercapacitors?" *Chemical Reviews*, vol. 104, pp. 4245–4269, 2004.

[6] E. Faggioli, P. Rena, V. Danel, X. Andrieu, R. Mallant, and H. Kahlen, "Supercapacitors for the energy management of electric vehicles," *Journal of Power Sources*, vol. 84, no. 2, pp. 261–269, 1999.

[7] R. Tummala, R. K. Guduru, and P. S. Mohanty, "Nanostructured Co_3O_4 electrodes for supercapacitor applications from plasma spray technique," *Journal of Power Sources*, vol. 209, pp. 44–51, 2012.

[8] Y. Hou, Y. Cheng, T. Hobson, and J. Liu, "Design and synthesis of hierarchical MnO_2 nanospheres/carbon nanotubes/conducting polymer ternary composite for high performance electrochemical electrodes," *Nano Letters*, vol. 10, no. 7, pp. 2727–2733, 2010.

[9] B. E. Conway, "Transition from 'supercapacitor' to 'battery' behavior in electrochemical energy storage," *Journal of the Electrochemical Society*, vol. 138, no. 6, pp. 1539–1548, 1991.

[10] T. Xue, C.-L. Xu, D.-D. Zhao, X.-H. Li, and H.-L. Li, "Electrodeposition of mesoporous manganese dioxide supercapacitor electrodes through self-assembled triblock copolymer templates," *Journal of Power Sources*, vol. 164, no. 2, pp. 953–958, 2007.

[11] B. E. Conway, V. Birss, and J. Wojtowicz, "The role and utilization of pseudocapacitance for energy storage by supercapacitors," *Journal of Power Sources*, vol. 66, no. 1-2, pp. 1–14, 1997.

[12] J. P. Zheng, P. J. Cygan, and T. R. Jow, "Hydrous ruthenium oxide as an electrode material for electrochemical capacitors," *Journal of the Electrochemical Society*, vol. 142, no. 8, pp. 2699–2703, 1995.

[13] J. Chang, W. Lee, R. S. Mane, B. W. Cho, and S.-H. Han, "Morphology-dependent electrochemical supercapacitor properties of indium oxide," *Electrochemical and Solid-State Letters*, vol. 11, no. 1, pp. A9–A11, 2008.

[14] I. Jung, J. Choi, and Y. Tak, "Nickel oxalate nanostructures for supercapacitors," *Journal of Materials Chemistry*, vol. 20, no. 29, pp. 6164–6169, 2010.

[15] O. Ghodbane, J.-L. Pascal, and F. Favier, "Microstructural effects on charge-storage properties in MnO_2-based electrochemical supercapacitors," *ACS Applied Materials & Interfaces*, vol. 1, no. 5, pp. 1130–1139, 2009.

[16] V. R. Shinde, S. B. Mahadik, T. P. Gujar, and C. D. Lokhande, "Supercapacitive cobalt oxide (Co_3O_4) thin films by spray pyrolysis," *Applied Surface Science*, vol. 252, no. 20, pp. 7487–7492, 2006.

[17] J. Yan, T. Wei, W. Qiao et al., "Rapid microwave-assisted synthesis of graphene nanosheet/Co_3O_4 composite for supercapacitors," *Electrochimica Acta*, vol. 55, no. 23, pp. 6973–6978, 2010.

[18] R. K. Selvan, I. Perelshtein, N. Perkas, and A. Gedanken, "Synthesis of hexagonal-shaped SnO_2 nanocrystals and SnO_2@C nanocomposites for electrochemical redox supercapacitors," *The Journal of Physical Chemistry C*, vol. 112, no. 6, pp. 1825–1830, 2008.

[19] J. P. Zheng and T. R. Jow, "High energy and high power density electrochemical capacitors," *Journal of Power Sources*, vol. 62, no. 2, pp. 155–159, 1996.

[20] J. P. Zheng, J. Huang, and T. R. Jow, "The limitations of energy density for electrochemical capacitors," *Journal of the Electrochemical Society*, vol. 144, no. 6, pp. 2026–2031, 1997.

[21] G. P. Wang, L. Zhang, and J. J. Zhang, "A review of electrode materials for electrochemical supercapacitors," *Chemical Society Reviews*, vol. 41, no. 2, pp. 797–828, 2012.

[22] M.-J. Deng, F.-L. Huang, I.-W. Sun, W.-T. Tsai, and J.-K. Chang, "An entirely electrochemical preparation of a nanostructured cobalt oxide electrode with superior redox activity," *Nanotechnology*, vol. 20, no. 17, Article ID 175602, 2009.

[23] Y. Liu, W. W. Zhao, and X. G. Zhang, "Soft template synthesis of mesoporous $Co_3O_4/RuO_2{\cdot}xH_2O$ composites for electrochemical capacitors," *Electrochimica Acta*, vol. 53, no. 8, pp. 3296–3304, 2008.

[24] C. Lin, J. A. Ritter, and B. N. Popov, "Characterization of sol-gel-derived cobalt oxide xerogels as electrochemical capacitors," *Journal of the Electrochemical Society*, vol. 145, no. 12, pp. 4097–4103, 1998.

[25] K. S. Novoselov, A. K. Geim, S. V. Morozov et al., "Electric field in atomically thin carbon films," *Science*, vol. 306, no. 5696, pp. 666–669, 2004.

[26] Y. Wang, Z. Q. Shi, Y. Huang et al., "Supercapacitor devices based on graphene materials," *The Journal of Physical Chemistry C*, vol. 113, no. 30, pp. 13103–13107, 2009.

[27] Y. Wang, C. Guan, K. Wang, C. X. Guo, and C. M. Li, "Nitrogen, hydrogen, carbon dioxide, and water vapor sorption

properties of three-dimensional graphene," *Journal of Chemical and Engineering Data*, vol. 56, no. 3, pp. 642–645, 2011.

[28] Y. Wang, C. X. Guo, J. Liu, T. Chen, H. Yang, and C. M. Li, "CeO_2 nanoparticles/graphene nanocomposite-based high performance supercapacitor," *Dalton Transactions*, vol. 40, no. 24, pp. 6388–6391, 2011.

[29] X. C. Dong, J. X. Wang, J. Wang et al., "Supercapacitor electrode based on three-dimensional graphene–polyaniline hybrid," *Materials Chemistry and Physics*, vol. 134, no. 2-3, pp. 576–580, 2012.

[30] C. X. Guo, F. P. Hu, X. W. Lou, and C. M. Li, "High-performance biofuel cell made with hydrophilic ordered mesoporous carbon as electrode material," *Journal of Power Sources*, vol. 195, no. 13, pp. 4090–4097, 2010.

[31] W. Zhou, J. Liu, T. Chen et al., "Fabrication of Co_3O_4-reduced graphene oxide scrolls for high-performance supercapacitor electrodes," *Physical Chemistry Chemical Physics*, vol. 13, no. 32, pp. 14462–14465, 2011.

[32] A. Pendashteh, M. F. Mousavi, and M. S. Rahmanifar, "Fabrication of anchored copper oxide nanoparticles on graphene oxide nanosheets via an electrostatic coprecipitation and its application as supercapacitor," *Electrochimica Acta*, vol. 88, pp. 347–357, 2013.

[33] S. X. Deng, D. Sun, C. H. Wu et al., "Synthesis and electrochemical properties of MnO_2 nanorods/graphene composites for supercapacitor applications," *Electrochimica Acta*, vol. 111, pp. 707–712, 2013.

[34] X. Dai, W. Shi, H. Cai, R. Li, and G. Yang, "Facile preparation of the novel structured α-MnO_2/graphene nanocomposites and their electrochemical properties," *Solid State Sciences*, vol. 27, pp. 17–23, 2014.

[35] X.-C. Dong, H. Xu, X.-W. Wang et al., "3D graphene-cobalt oxide electrode for high-performance supercapacitor and enzymeless glucose detection," *ACS Nano*, vol. 6, no. 4, pp. 3206–3213, 2012.

[36] X. Wang, S. Liu, H. Wang, F. Tu, D. Fang, and Y. Li, "Facile and green synthesis of Co_3O_4 nanoplates/graphene nanosheets composite for supercapacitor," *Journal of Solid State Electrochemistry*, vol. 16, no. 11, pp. 3593–3602, 2012.

[37] G. He, J. Li, H. Chen et al., "Hydrothermal preparation of Co_3O_4@graphene nanocomposite for supercapacitor with enhanced capacitive performance," *Materials Letters*, vol. 82, pp. 61–63, 2012.

[38] Y. Wang, J. H. Liu, K. Wang, T. Chen, X. Tan, and C. M. Li, "Hydrogen storage in Ni-B nanoalloy-doped 2D graphene," *International Journal of Hydrogen Energy*, vol. 36, no. 20, pp. 12950–12954, 2011.

[39] J. Li, H. Xie, Y. Li, J. Liu, and Z. Li, "Electrochemical properties of graphene nanosheets/polyaniline nanofibers composites as electrode for supercapacitors," *Journal of Power Sources*, vol. 196, no. 24, pp. 10775–10781, 2011.

[40] S.-J. Bao, C. M. Li, C.-X. Guo, and Y. Qiao, "Biomolecule-assisted synthesis of cobalt sulfide nanowires for application in supercapacitors," *Journal of Power Sources*, vol. 180, no. 1, pp. 676–681, 2008.

[41] R. Z. Ma, J. Liang, B. Q. Wei, B. Zhang, C. L. Xu, and D. H. Wu, "Study of electrochemical capacitors utilizing carbon nanotube electrodes," *Journal of Power Sources*, vol. 84, no. 1, pp. 126–129, 1999.